View metadata, citation and similar papers at core.ac.uk
brought to you by CORE
provided by Elsevier - Publisher Connector

Cell

Premature Activation of the SLX4 Complex by Vpr Promotes G2/M Arrest and Escape from Innate Immune Sensing

Nadine Laguette,[1,*] Christelle Brégnard,[1] Pauline Hue,[1] Jihane Basbous,[2] Ahmad Yatim,[1] Marion Larroque,[2] Frank Kirchhoff,[3] Angelos Constantinou,[2] Bijan Sobhian,[1] and Monsef Benkirane[1,*]
[1]Institut de Génétique Humaine, Laboratoire de Virologie Moléculaire
[2]Laboratoire Instabilité du Génome et Cancer
CNRS UPR1142, Montpellier 34000, France
[3]Institute of Molecular Virology, Ulm University Medical Center, 81089 Ulm, Germany
*Correspondence: nadine.laguette@igh.cnrs.fr (N.L.), monsef.benkirane@igh.cnrs.fr (M.B.)
http://dx.doi.org/10.1016/j.cell.2013.12.011

SUMMARY

The HIV auxiliary protein Vpr potently blocks the cell cycle at the G2/M transition. Here, we show that G2/M arrest results from untimely activation of the structure-specific endonuclease (SSE) regulator SLX4 complex (SLX4com) by Vpr, a process that requires VPRBP-DDB1-CUL4 E3-ligase complex. Direct interaction of Vpr with SLX4 induced the recruitment of VPRBP and kinase-active PLK1, enhancing the cleavage of DNA by SLX4-associated MUS81-EME1 endonucleases. G2/M arrest-deficient Vpr alleles failed to interact with SLX4 or to induce recruitment of MUS81 and PLK1. Furthermore, knockdown of SLX4, MUS81, or EME1 inhibited Vpr-induced G2/M arrest. In addition, we show that the SLX4com is involved in suppressing spontaneous and HIV-1-mediated induction of type 1 interferon and establishment of antiviral responses. Thus, our work not only reveals the identity of the cellular factors required for Vpr-mediated G2/M arrest but also identifies the SLX4com as a regulator of innate immunity.

INTRODUCTION

Many viruses, including HIV-1, perturb the progression through the host cell cycle. This is achieved through subversion of the boundaries between the DNA replication step (S), segregation of sister chromatids (mitosis), and the gap phases (G1 and G2) (Davy and Doorbar, 2007). Manipulation of the host cell cycle by HIV-1 is achieved through the highly conserved 96 amino acid Vpr protein that causes a potent cell-cycle arrest at the G2 to mitosis transition (G2/M) in most cycling eukaryotic cells (Di Marzio et al., 1995; He et al., 1995; Jowett et al., 1995; Re et al., 1995; Rogel et al., 1995). G2/M arrest by Vpr has been proposed to rely on Vpr-induced activation of the DNA damage surveillance proteins ataxia-telangiectasia-mutated kinase (ATM) and ATM and Rad3-related kinase (ATR) that detect DNA lesions and trigger downstream signaling cascades (Poon et al., 1997; Roshal et al., 2003). Activation of ATM and ATR may cause cell-cycle arrest, which, in the absence of HIV-1 infection, allows time for repair. Importantly, although Vpr expression results in formation of breast cancer susceptibility protein 1 (BRCA1) and γH2ax foci (Zimmerman et al., 2004), it remains unclear whether Vpr induces double-strand breaks (DSB) (Lai et al., 2005; Tachiwana et al., 2006) and whether this damage would be the trigger for cell-cycle arrest. A proposed scenario is that Vpr activates the G2/M checkpoint through a replication stress-dependent pathway (Li et al., 2010). Cellular partners of Vpr that may contribute to G2/M arrest have been proposed, yet no consensus has been reached apart from the absolute requirement for the VPRBP-DDB1-CUL4 E3-ligase complex (Belzile et al., 2007; DeHart et al., 2007; Hrecka et al., 2007; Le Rouzic et al., 2007; Tan et al., 2007; Wen et al., 2007).

Homologous recombination (HR) is a crucial repair pathway in mammalian cells, employed to repair DSB and collapsed replication forks. HR allows accurate repair using the sister chromatid as a template and leads to the formation of four-way DNA structures, Holliday junctions (HJ), that must be removed prior to chromosome segregation. In somatic cells, the favored pathway to remove HJ relies on Bloom-related helicases that dissolve HJ in a nonendonucleolytic fashion that prevents sister chromatid exchanges (SCE) (Wu and Hickson, 2003). Failure to dissolve HJ may be rescued by the resolution pathway that relies on structure-specific endonuclease (SSE). In human cells, MUS81-EME1, SLX1-SLX4, and GEN1 have been involved in this process (Schwartz and Heyer, 2011). Though these proteins display different activities in vitro, in vivo SLX4 acts as a central scaffold that, in addition to interacting with SLX1, also recruits MUS81-EME1 and ERCC1-ERCC4^{XPF} and other proteins involved in DNA metabolism (Fekairi et al., 2009; Kim et al., 2013; Muñoz et al., 2009; Svendsen et al., 2009). However, because the action of these proteins may lead to the formation of SCE and therefore result in loss of heterozygosity (LOH), their action is kept under tight control both under physiological conditions and following DNA damage (Dehe et al., 2013; Gallo-Fernández et al., 2012; Matos et al., 2011, 2013; Saugar et al., 2013; Szakal and Branzei, 2013).

CrossMark

Processing of collapsed replication forks by MUS81-EME1 is essential to the maintenance of genomic integrity (Beck et al., 2012; Fugger et al., 2013; Hanada et al., 2007). In addition, absence of MUS81-EME1 may result in failure to remove ultrafine DNA bridges (UFBs) and subsequent common fragile site (CFS)-associated chromosomal instability (Chan et al., 2009; Naim et al., 2013; Wechsler et al., 2011; Ying et al., 2013). Similarly, Mus81-Mms4^{EME1} activation operates as a fail-safe mechanism in yeast to repair stalled replication forks that escape other repair pathways (Dehe et al., 2013; Matos et al., 2013; Saugar et al., 2013). Importantly, because untimely or persistent endonuclease activation may lead to abnormal processing of replication forks (Gallo-Fernández et al., 2012; Matos et al., 2013; Szakal and Branzei, 2013), even in the case of replication stress, full acquisition of endonuclease activity by Mus81-Mms4^{EME1} occurs after completion of bulk DNA synthesis (Dehe et al., 2013; Saugar et al., 2013). Recent work has established that Mus81-Mms4^{EME1} activation is mostly confined to the G2/M transition through Cdc5^{PLK1} phosphorylation of Mms4^{EME1} in budding yeast (Gallo-Fernández et al., 2012; Matos et al., 2013; Saugar et al., 2013) or Cdc2^{CDK1} in fission yeast (Dehe et al., 2013), a process speculated to be similar to the one observed in mammalian cells in which activation of MUS81-EME1 requires phosphorylation of EME1 by PLK1 (Matos et al., 2011).

Here, we addressed both the molecular mechanism underlying Vpr-mediated G2/M arrest and its significance for HIV-1 life cycle. Using a biochemical approach, we found that the SSE regulator SLX4com interacts with Vpr. We show that Vpr causes untimely activation of SLX4-bound MUS81-EME1 through the recruitment of VPRBP and kinase-active PLK1. Importantly, silencing of subunits of the SLX4com impedes Vpr-induced G2/M arrest. Finally, we show that the targeting of active SLX4com by Vpr to HIV-1 DNA is a viral strategy to avoid innate immune sensing.

RESULTS

Vpr Interacts with the SSE Regulator Complex SLX4

In order to identify cellular partners involved in Vpr-mediated G2/M arrest, we established a stable monocytic cell line expressing FLAG- and HA-tagged Vpr (iF/H-Vpr) under the control of a tetracycline-inducible promoter (THP-1-iF/H-Vpr). THP-1-iF/H-Vpr or parental THP-1 cells were grown, induced to express iF/H-Vpr, and harvested before G2/M arrest (Figures 1A and S1A available online). Following tandem affinity purification, immunoprecipitated material was resolved on SDS-PAGE and silver-stained (Figure 1B), and protein partners were identified by mass spectrometry (MS). Previously identified Vpr partners were recovered, including subunits of the VPRBP-DDB1-CUL4 E3-ligase complex and UNG2 (Casey et al., 2010) (Figures 1B and S1B), validating our experimental approach. Interestingly, the SSE ERCC1-ERCC4 and MUS81-EME1, together with the SLX4 scaffold protein, were recovered, as well as the poorly characterized TSPYL1 and C20orf94 subunits of the SLX4com (Figures 1B and S1B).

We first confirmed the interaction between iF/H-Vpr and the identified SLX4com subunits by western blot (WB) (Figure 1C). Importantly, this interaction is specific to Vpr because immunopurified HIV-2 viral accessory protein Vpx, which is closely related to Vpr (Tristem et al., 1992), failed to interact with the SLX4com (Figure S1B). In addition, GFP-tagged SLX4 (GFP-SLX4), which is expressed in HeLa cells, colocalized with iF/H-Vpr (Figure S1C), providing further evidence for a physical interaction. Interaction between Vpr and SLX4 was also observed in the presence of 0.1 mg/ml ethidium bromide and 0.1 U/μl DNaseI (Figure S1D), ruling out the requirement for a DNA intermediate. Next, in vitro interaction experiments were performed using recombinant glutathione S-transferase-tagged Vpr (GST-Vpr) and 6xHistidine-tagged subunits of the SLX4com (HIS_6-C20orf94, HIS_6-MUS81, and HIS_6-EME1) or the C-terminal SLX1 binding domain (SBD) of SLX4 (HIS_6-SBD) (Figure S1E). GST-tagged SLX1 (GST-SLX1) was used as a positive control. Direct interaction was only observed between HIS_6-SBD and GST-Vpr (Figures 1D and S1F; data not shown). Altogether, these results demonstrate that Vpr directly interacts with the C terminus of SLX4.

Because direct interaction between VPRBP and Vpr is required for Vpr-mediated G2/M arrest (Zhao et al., 1994), we asked whether VPRBP, Vpr, and subunits of the SLX4com assemble into a single complex. To this aim, glycerol gradient sedimentation of FLAG-purified iF/H-Vpr was performed, followed by WB analysis of collected fractions. Figure 1E shows an overlap of protein distribution along the gradient for all tested subunits. In addition, reciprocal immunoprecipitations (re-IPs) were performed (Figure 1F, left) using extracts prepared from cells expressing both FLAG-tagged SLX4 (FLAG-SLX4) and HA-tagged Vpr under the control of a tetracycline-inducible promoter (iHA-Vpr). Cell extracts were first subjected to FLAG-IP followed by Flag-peptide elution under native conditions. Immunopurified material was further subjected to HA-IP prior to analysis by WB, showing that all tested subunits of the SLX4com and VPRBP copurified with Vpr (Figures 1F and S1G). Taken together, the glycerol gradient velocity analysis and re-IPs strongly suggest that SLX4com subunits, VPRBP, and Vpr assemble in a single complex.

Because previous work did not identify VPRBP as a subunit of the SLX4com, we further explored this interaction in the presence and absence of Vpr. To this aim, immunoprecipitation (IP) of FLAG-tagged VPRBP (FLAG-VPRBP) was performed in the presence or absence of iHA-Vpr. The levels of SLX4, ERCC4, and MUS81 associated with VPRBP were significantly enhanced in Vpr-expressing cells (Figure 1G). This shows that VPRBP interacts with the SLX4com and that Vpr enhances this interaction.

Vpr Causes Untimely Activation of SLX4-Associated MUS81-EME1

We next wished to uncover whether Vpr expression would impact on SLX4com activity. We first performed WB analysis of whole-cell extracts (WCE) from stable HeLa cells induced to express iF/H-Vpr (HeLa-iF/H-Vpr) for 0, 2, 4, 8, 16, and 24 hr (Figure 2A). We observed that the levels of EME1 and MUS81 decreased prior to G2/M arrest (4–8 hr). Conversely, the levels of PLK1 and of its kinase-active Threonine 592-phosphorylated form (pPLK1)—known to regulate MUS81-EME1 activity through EME1 phosphorylation—increased before G2/M arrest. This raised the hypothesis that Vpr expression may modulate MUS81-EME1 activity through PLK1 activation prior to cell-cycle

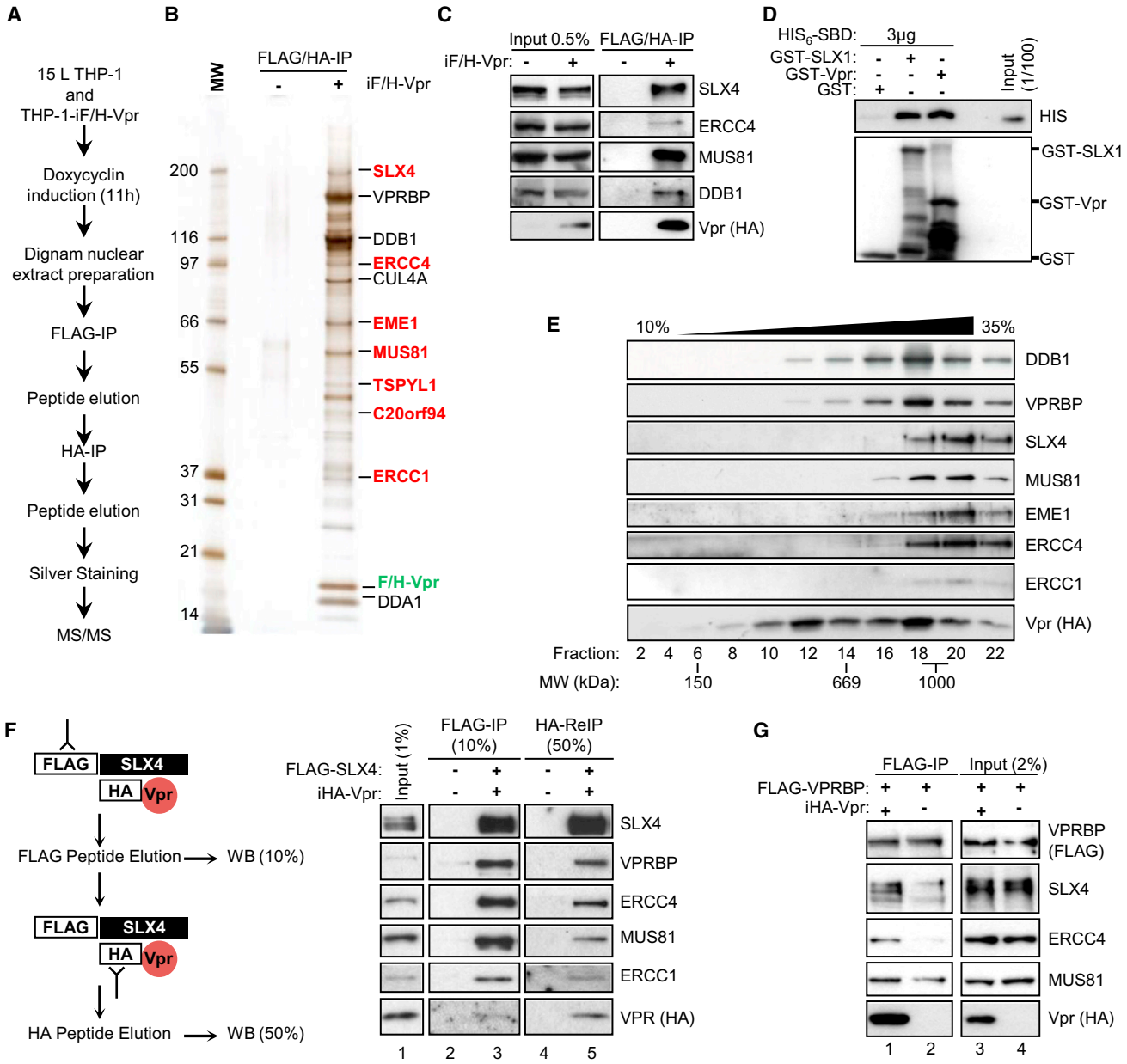

Figure 1. HIV Vpr Directly Interacts with the C-Terminal Domain of SLX4 and Recruits VPRBP

(A) Experimental scheme for (B) and (C).

(B) iF/H-Vpr was immunopurified as in (A), separated on SDS-PAGE, and silver stained. Major previously described Vpr partners (black), iF/H-Vpr (green), and SLX4com subunits (red) are indicated. MW, molecular weight (kDa).

(C) Input and eluates prepared as in (A) were analyzed by WB using indicated antibodies.

(D) In vitro interaction assay using HIS_6-tagged SLX1 binding domain of SLX4 (HIS_6-SBD), GST-SLX1, GST-Vpr, and GST. GST pulled-down material was analyzed by WB using anti-His and anti-GST antibodies. Additional bands, degradation products of recombinant proteins.

(E) FLAG-purified iF/H-Vpr was peptide eluted and subjected to glycerol-gradient sedimentation. Collected fractions were analyzed by WB using indicated antibodies.

(F) FLAG-SLX4 was purified from 293T cells in the presence of iHA-Vpr (8 hr induction). Peptide-eluted material was further HA immunopurified. Input material and eluates were analyzed by WB using indicated antibodies.

(G) FLAG-VPRBP was immunopurified in the presence or absence of iHA-Vpr (8 hr induction) and was peptide eluted. Eluates and input material were analyzed by WB using indicated antibodies.

See also Figure S1.

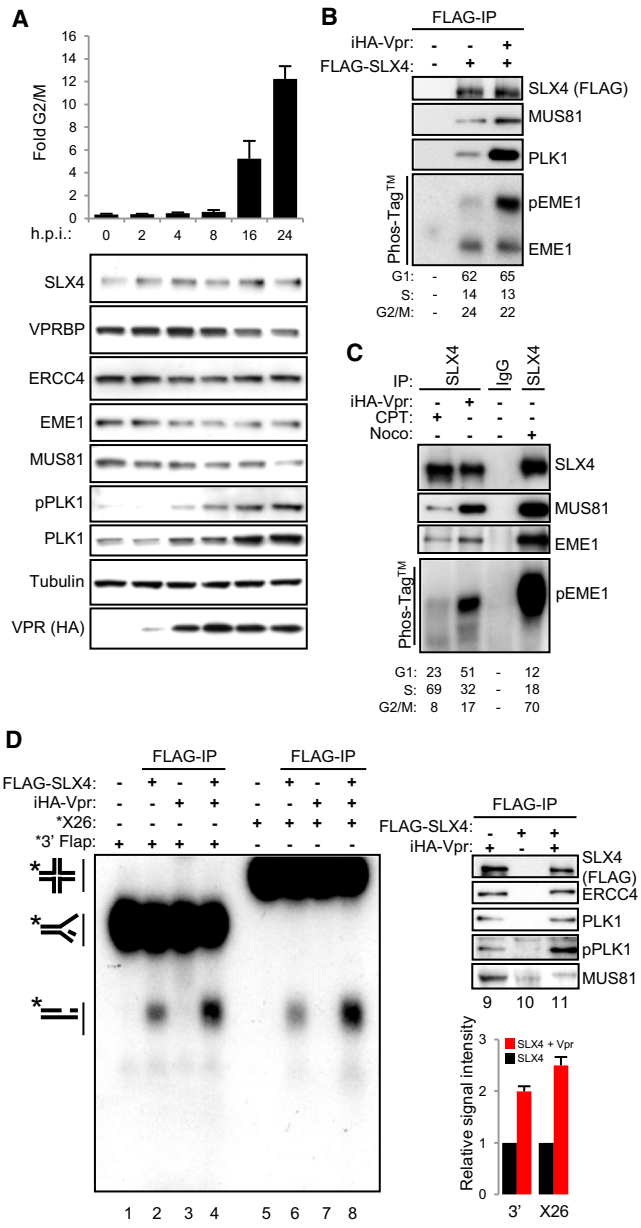

Figure 2. HIV Vpr Activates SLX4-Bound MUS81-EME1 through PLK1 Phosphorylation of EME1

(A) HeLa-iF/H-Vpr were induced to express Vpr for the indicated time prior to cell-cycle analysis using DAPI nuclear staining (top) and WCE and analysis by WB using indicated antibodies (bottom). h.p.i., hr postinduction.

(B) FLAG-SLX4 was immunopurified from 293T cells expressing or not expressing Vpr for 4 hr. Eluates were analyzed by SDS-PAGE or Phos-Tag and WB using indicated antibodies. Cell-cycle distribution analyzed as in (A) is indicated.

(C) HeLa-iF/H-Vpr cells were either induced to express Vpr for 8 hr or treated with 0.5μg/ml Noco or 50 nM CPT prior to whole-cell extraction and IP using anti-SLX4 or IgG. Immunoprecipitates were analyzed as in (B).

(D) FLAG-SLX4 was immunopurified from 293T cells in the presence or absence of iHA-Vpr. Cleavage of radiolabeled 3′ flap and X26 substrates was analyzed by autoradiography. Right: WB analysis of samples. Graph shows mean (± SD) cleavage efficiency in the presence of Vpr relative to in the absence of Vpr (n = 3).

See also Figure S2.

arrest. We therefore investigated the phosphorylation status of EME1 within the SLX4com. To this aim, FLAG-SLX4 was immunopurified from 293T cells in the absence of Vpr or following 4 hr of Vpr induction (Figure 2B). Using Phos-tag gels that allow the separation of phosphorylated forms of a protein, we observed that the expression of Vpr caused the accumulation of slower migrating bands (pEME1) associated with SLX4 (Figures 2B and S2A). Furthermore, expression of Vpr caused an increased recruitment of both PLK1 and pPLK1 to SLX4 (Figures 2B and S2A). Nocodazole (Noco) treatment was included as a control since it was previously shown to induce PLK1-dependent phosphorylation of EME1 (Figure S2A). Similarly, IP of FLAG-MUS81 showed that, although Vpr did not affect MUS81-EME1 interaction (Figure S2B, left), Vpr expression enhanced the phosphorylation of EME1 within the MUS81-EME1 complex (Figure S2B, right). Importantly, phosphatase treatment of immunoprecipitates prior to migration on Phos-tag gels lead to disappearance of slower migrating bands, confirming that those correspond to phosphorylated forms of EME1 (Figure S2B; data not shown). Altogether, these data suggest that Vpr induces the recruitment of PLK1 and its kinase active form to SLX4com, resulting in increased phosphorylation of EME1. Importantly, although Vpr-mediated remodeling of the SLX4com can be witnessed after 4 hr of Vpr induction (Figures 2B, S2A, and S2B), 16 to 24 hr induction of Vpr is required for G2/M arrest (Figure 2A). This shows that Vpr-mediated remodeling of the SLX4com precedes G2/M arrest.

It has recently been shown that activation of MUS81-EME1 is confined to late G2/early mitosis to allow processing of late DNA joint molecules that would otherwise impede the correct segregation of chromosomes. To establish at which stage of the cell cycle pPLK1 and MUS81-EME1 associate with SLX4 in mammalian cells, cells were arrested in G1/S, S/G2, and mitosis using 2 mM thymidine (Thym), 50 nM camptothecin (CPT), or 0.5 μg/ml nocodazole, respectively. WB analysis of FLAG-SLX4 immunopurified in these conditions showed increased recruitment of pEME1 and PLK1 to SLX4 only upon nocodazole treatment, indicating that, in mammalian cells, SLX4com assembly and EME1 phosphorylation take place during mitosis (Figure S2C). To rule out the possibility that Vpr-mediated activation of the SLX4com is a consequence of G2/M arrest, we performed a similar experiment, including cells that were harvested 8 hr after Vpr induction. Vpr induced the recruitment of MUS81 and pEME1 to the SLX4 platform prior G2/M arrest (Figure 2C). Consistently, Vpr induced the accumulation of PLK1 in WCE during G1/S (Figure S2D). Thus, our data suggest that Vpr induces untimely activation of the SLX4com.

To confirm this hypothesis, we assessed the endonuclease activity associated with SLX4 in the presence or absence of Vpr toward 3′ flap and X26 (mobile HJ that includes a 26 bp homologous core) radiolabelled DNA substrates. Human MUS81-EME1 have been shown to display highest processing activity against 3′ flap substrates and low activity against X26, whereas human SLX4-SLX1 target X26 (Sengerová et al., 2011; Svendsen and Harper, 2010). FLAG-SLX4 was purified following 6 hr of iHA-Vpr induction, and bead-bound FLAG-SLX4 complexes were tested in in vitro cleavage assays. FLAG-SLX4 purified in the presence of Vpr displayed increased cleavage ability toward 3′ flap

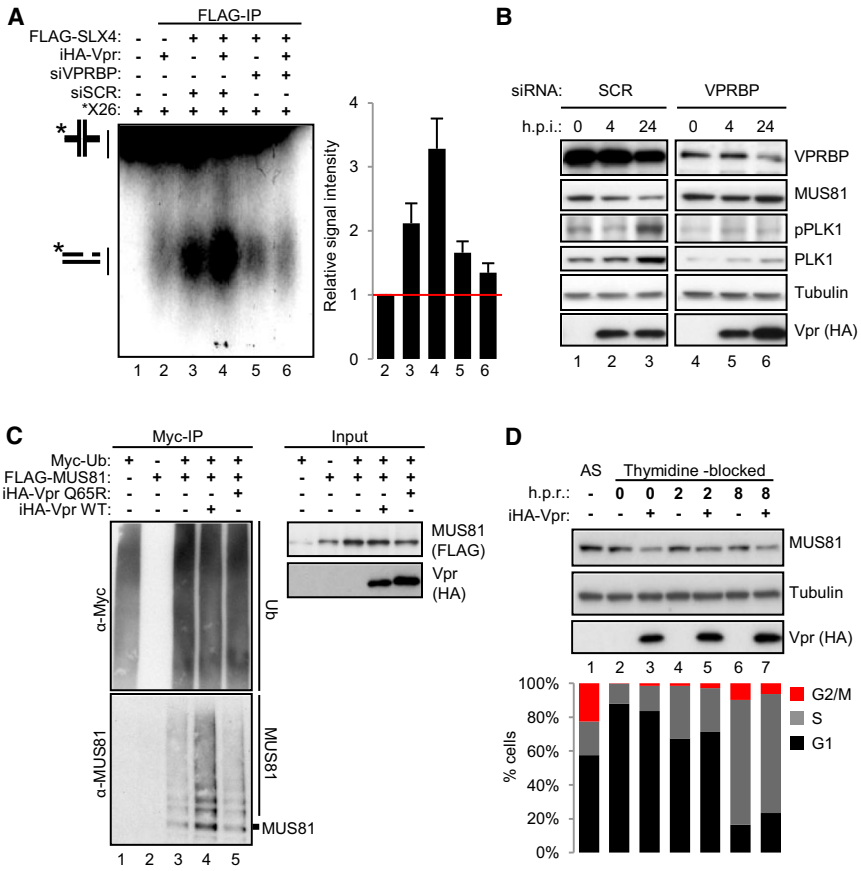

Figure 3. VPRBP Is Required for Vpr-Induced Activation of the SLX4com and Modulation of MUS81 Levels

(A) Experimental scheme was as in Figure 2E, except that 293T cells were either transfected with siSCR or siVPRBP prior to whole-cell extraction. Mean (±SD) cleavage efficiency relative to lane 2 (n = 3).

(B) HeLa-iF/H-Vpr were transfected with siSCR or siVPRBP 24 hr before induction of iF/H-Vpr expression for indicated time. WCE were analyzed by WB using indicated antibodies.

(C) Myc-Ub was coexpressed with FLAG-MUS81 and iHA-Vpr or iHA-VprQ65R in 293T cells. Vpr expression was induced for 16 hr, and 50 nM MG132 was added to the media 2 hr prior to whole-cell extraction and Myc-IP. Immunoprecipitates and inputs were analyzed by WB using indicated antibodies.

(D) HeLa-iF/H-Vpr were treated for 20 hr with 2 mM thymidine prior to release in complete media. Cell cycle was analyzed using DAPI nuclear staining (bottom), and WCE were analyzed by WB using indicated antibodies. h.p.r., hr postrelease.

See also Figure S3.

and X26 as compared to FLAG-SLX4 purified in the absence of Vpr (Figure 2D compare lanes 2–4 and lanes 6–8). To further examine the contribution of the MUS81-EME1 module, we performed similar experiments after MUS81 knockdown (Figures S2E–S2G). We thereby observed that MUS81 silencing resulted in loss of Vpr-mediated increase of SLX4com activity toward X26 and 3′ flap substrates (Figures S2E and S2F, compare lanes 5–7 to 8–10). This suggests that Vpr-mediated increase of SLX4com activity mostly results from activation of the MUS81-EME1 module. Altogether, our data indicate that Vpr expression causes precocious activation of SLX4-associated MUS81-EME1.

VPRBP Is Required for Vpr-Mediated Activation of the SLX4 Complex and Modulation of MUS81 Levels

Because VPRBP, Vpr, and SLX4com assemble into a single complex (Figure 1) and, given that VPRBP is required for Vpr-mediated G2/M arrest, we explored its role in Vpr-mediated activation of the SLX4com. In vitro nuclease activity assays were performed using FLAG-SLX4 immunopurified in the presence or absence of Vpr in nontargeting (SCR) small interfering RNA (siRNA) or siVPRBP-treated cells (Figures 3A and S3A). Silencing of VPRBP abolished the Vpr-dependent enhancement of SLX4com cleavage activity toward X26 (Figure 3A, compare lanes 3–4 to 5–6). We next wanted to assess whether VPRBP is required for PLK1 activation. To this aim, HeLa-iF/H-Vpr cells were transfected with siVPRBP or siSCR and subsequently induced to express Vpr. Levels of PLK1 and pPLK1 were assessed by WB. Figure 3B shows that silencing of VPRBP abolished Vpr-dependent accumulation of PLK1 and pPLK1. This supports the finding that VPRBP is required for the activation of SLX4-associated MUS81-EME1.

In agreement with results shown in Figure 2A, Vpr induced a decrease of MUS81 levels that is abolished upon VPRBP silencing (Figures 3B and S3B). This raised the hypothesis that VPRBP may be involved in regulating the levels of MUS81. Thus, we assessed the ubiquitination of MUS81 in the presence or absence of Vpr. As a control, the ubiquitination of MUS81 was also assessed in the presence of a Vpr allele with arginine in place of glutamine at position 65 that does not interact with VPRBP (VprQ65R). IP of Myc-Ub-associated MUS81 showed that the expression of WT Vpr, but not of VprQ65R, caused increased ubiquitination of MUS81 (Figure 3C, compare lanes 4–3 and lanes 5–4). This shows that interaction of VPRBP with Vpr is involved in MUS81 ubiquitination.

Finally, to rule out that MUS81 degradation may be a consequence of the G2/M arrest, we first treated cells with nocodazole for up to 24 hr. WB analysis showed that nocodazole treatment did not induce a significant modulation of MUS81 levels (Figure S3C). Next, HeLa cells were blocked in G1 using Thymidine and induced to express Vpr 8 hr prior to release and harvested 2 hr and 8 hr postrelease. WCE were analyzed by WB. In G1-arrested cells, Vpr expression induced a decrease of MUS81 levels that persisted in S phase (Figure 3D). Of note, in the absence of Vpr, the levels of MUS81 do not vary in a cell-cycle-dependent manner (Figure S3C). This shows that Vpr-mediated MUS81 decrease did not result from G2/M arrest. Altogether, our data indicate that the recruitment of VPRBP to the SLX4com is

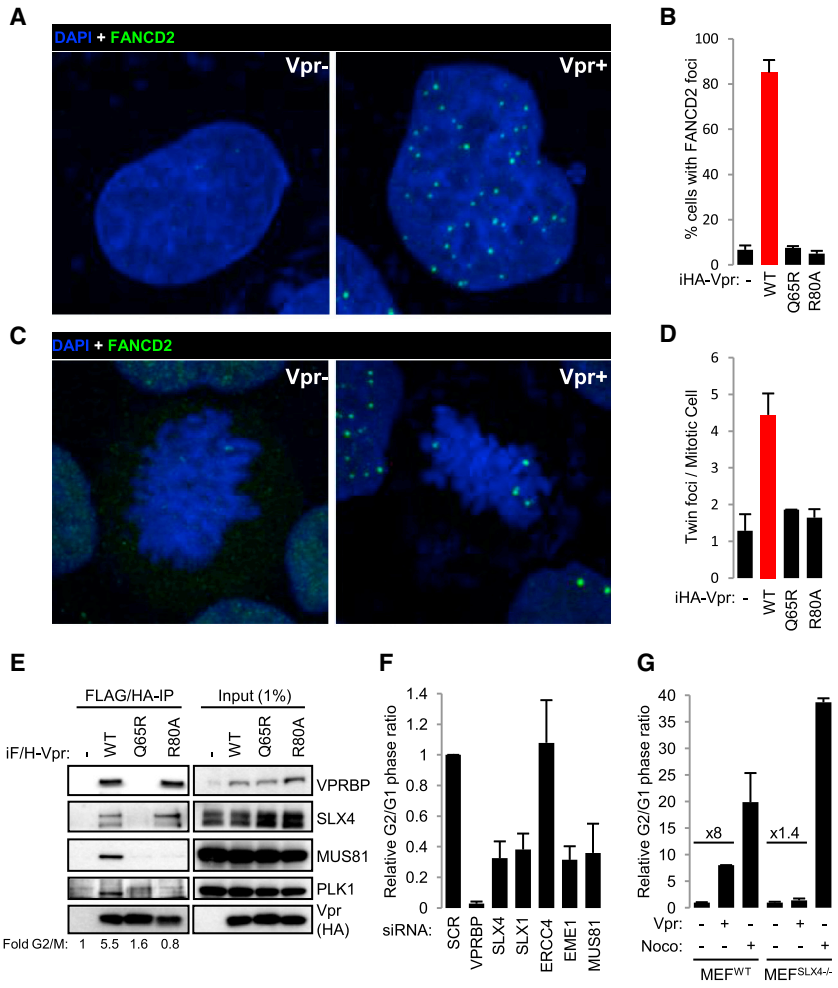

Figure 4. Premature Vpr-Induced MUS81-EME1 Activation Results in FANCD2 Foci Accumulation and G2/M Arrest

(A–D) HeLa cells were induced to express Vpr (A and C, right) or not (A and C, left) for 24 hr prior to immunofluorescence analysis using anti-FANCD2 antibody and DAPI staining. Images show representative cells entering mitosis (C) or not (A). Total number of cells with FANCD2 foci (C) and the number of twin foci per mitotic cell (B) upon Vpr expression were counted in at least 400 cells per condition. Graphs show mean ± SD.

(E) iF/H-Vpr, iF/H-VprQ65R, and iF/H-VprR80A were tandem affinity purified from THP-1 cells (11 hr induction) and analyzed by WB using indicated antibodies. Fold G2/M is indicated.

(F) HeLa cells were treated as in Figure 3B, except that siRNAs against SLX4, SLX1, ERCC4, EME1, and MUS81 were also used. The cell cycle was analyzed by Flow cytometry measuring incorporation of EdU and nuclear content (DAPI). Relative G2/G1 ratio is plotted. Graph shows mean ± SD (n = 3).

(G) Cell-cycle analysis was performed using DAPI nuclear staining in MEF and MEF$^{SLX4-/-}$-expressing Vpr or treated with 0.5μg/ml Noco for 24 hr. Graph shows mean ± SD (n = 3).

See also Figure S4.

required for Vpr-mediated activation of the SLX4com and regulation of MUS81 levels.

Premature MUS81-EME1 Activation by Vpr Results in FANCD2 Foci Accumulation and G2/M Arrest

Vpr-induced premature activation of the SLX4-bound MUS81-EME1 may lead to faulty cleavage of replication intermediates. Conversely, decreased levels of MUS81 could prevent the processing of crossover intermediates before entry into mitosis. Deregulation of MUS81-EME1 by Vpr may thus lead to accumulation of damaged DNA and subsequent genomic instability. Because ongoing replication stress and persistence of unresolved replication intermediates can be marked by an accumulation of FANCD2 foci (Naim and Rosselli, 2009), these were quantified by immunofluorescence staining in HeLa-iF/H-Vpr 24 hr post-Vpr induction. We observed a stark increase of FANCD2 foci upon expression of Vpr (Figures 4A, S4A, and S4B). Additionally, the number of FANCD2 twin foci was also dramatically increased in Vpr-positive cells that undergo chromosome condensation (Figures 4B–4D). These increases were not observed in cells expressing VprQ65R or VprR80A (alanine to arginine substitution at position 80), suggesting that these Vpr mutants fail to modulate MUS81-EME1 activity (Figures 4C and 4D).

Consistently, both VprQ65R and VprR80A have been documented to fail to induce G2/M arrest. However, mutation R80A does not disrupt interaction with VPRBP (Belzile et al., 2007; DeHart et al., 2007). We thus tested these Vpr alleles for their ability to interact with members of the SLX4com. To this aim, cells expressing F/H-iVpr, F/H-iVprQ65R, or F/H-iVprR80A were harvested prior to G2/M arrest, WCE prepared, and subjected to tandem-affinity purification prior to analysis by WB (Figures 4E and S4C). Consistent with published observations, VprQ65R failed to interact with VPRBP. Interestingly, VprQ65R failed to interact with SLX4, MUS81, and PLK1. In contrast, VprR80A interacted with VPRBP and SLX4 but failed to recruit both MUS81 and PLK1 (Figures 4E and S4C). Thus, sole interaction of Vpr with VPRBP and SLX4 is not sufficient to induce G2/M arrest, and recruitment of PLK1 and MUS81-EME1 is mandatory for this Vpr-associated activity. Altogether, these observations suggest that Vpr-induced modulation of MUS81-EME1 activity may result in replication stress.

To further investigate the contribution of subunits of the SLX4com to Vpr-induced G2/M arrest, we used siRNAs targeting VPRBP, SLX4, SLX1, ERCC4, EME1, and MUS81 (Figures S4D and S4F) in HeLa-iF/H-Vpr prior to 24 hr Vpr induction. G2/M arrest (Figures 4F and S4D–S4G) and the percentage of S phase cells (Figures S4G and S4H) were measured. As control, siSCR did not influence Vpr's ability to induce G2/M arrest. Silencing of SLX4, SLX1, EME1, and MUS81, but not ERCC4, caused a reduction of Vpr-induced G2/M arrest. The requirement for SLX1 is congruent with the ability of Vpr to increase

processing of X26 substrates. In this assay, silencing of VPRBP caused a more profound disruption of Vpr-induced G2/M arrest (Figures 4F and S4G) than silencing of SLX4com subunits, mirroring siRNA efficiency. Accordingly, Vpr-induced G2/M arrest is abolished in mouse embryonic fibroblasts (MEF) knocked out for SLX4 ($MEF^{SLX4-/-}$). Furthermore, when siSLX4-treated HeLa cells are engineered to express SLX4, Vpr-induced G2/M arrest is restored (Figure S4H).

Of note, modifications of the distribution of cells in S phase were observed upon siRNA treatment (Figures S4G–S4I). Nocodazole treatment of cells knocked down for VPRBP, SLX4, SLX1, and EME1 demonstrated that these cells were not blocked at the G1/S transition (data not shown), ruling out the possibility that the inability of Vpr to induce G2/M arrest in these cells may be an indirect consequence of a G1/S block. In contrast, MUS81-silenced cells were blocked at the G1/S transition, indicating that MUS81 is required to proceed into the S phase. Altogether, our data confirm the importance of VPRBP in the regulation of MUS81-EME1 activity and the requirement for SLX4com activation for Vpr-induced G2/M arrest.

Vpr Activates the SLX4 Complex to Avoid Triggering Innate Immunity

SLX4 (FANCP) belongs to the Fanconi Anemia (FA) family of proteins. A hallmark of FA, besides heightened cancer susceptibility and bone marrow failure, is the abnormal production of interferon (IFN) and proinflammatory cytokines (Fagerlie et al., 2004). Interestingly, Vpr has been shown to modulate IFN responses (Doehle et al., 2009; Okumura et al., 2008). In light of recent findings demonstrating that viral manipulation of nucleases plays a role in the control of innate immune signaling (Yan et al., 2010), we hypothesized that the SLX4com could be subverted by Vpr to avoid eliciting innate immune responses. HeLa cells were transfected with siSCR, siMUS81, siVPRBP, and siSLX4 prior to a single-round infection assay using a vesicular stomatitis virus G protein (VSV-G)-pseudotyped HIV-1 molecular clone harboring a IRES-eGFP sequence as a reporter (HIV-GFP) and type 1 IFN (IFNα and IFNβ) and IFN-stimulated gene (ISG) MxA mRNA quantification by qPCR (Figures 5A and S5A). In this experimental setting, the percentage of infected cells was not significantly modified by siRNA treatment (Figure S5B). Infection of MUS81, VPRBP, and SLX4 knockdown cells resulted in induction of IFNα, IFNβ mRNA, and type 1 IFN response as demonstrated by induction of MxA mRNA (Figure 5A). This indicates that MUS81, SLX4, and VPRBP are required for HIV-1 escape from innate immune sensing. In addition, infection with VSV-G-pseudotyped HIVΔVpr-GFP (HIV-GFP with a deletion of the *vpr* open reading frame) caused up to 3-fold increase of IFNα, IFNβ, and MxA mRNAs as compared to infection with HIV-GFP (Figure 5B).

Because the SLX4com is recruited to damaged DNA, we explored whether SLX4com subunits are able to bind HIV-1 reverse transcripts. IP of FLAG-SLX4 from HIV-1-infected cells and quantification of FLAG-SLX4-bound HIV-1 DNA by qPCR showed significant binding of HIV-1 DNA (Figure 5C). Of note, binding of HIV-1 DNA was also observed in FLAG-MUS81 immunoprecipitates (Figure S5C). To confirm that HIV-1 DNA bound to SLX4 was a product of viral reverse transcription, we performed a similar experiment using a reverse transcription inhibitor (AZT). Upon AZT treatment, the binding of SLX4 to viral DNA was abolished (Figure 5D).

To establish whether Vpr is involved in SLX4 binding to HIV-1 DNA, we analyzed SLX4 binding to viral DNA in the presence and absence of Vpr. We found that, despite similar levels of input viral DNA (Figure 5E, left) and similar levels of immunoprecipitated endogenous SLX4 (Figure S5D), HIV DNA was only recovered after infection with HIV-GFP (Figure 5E, right). This suggests that Vpr is required for SLX4 binding to HIV-1 DNA. Based on the above information, one can hypothesize that Vpr induces SLX4 to bind and process HIV-1 DNA in order to avoid excess viral DNA accumulation that would otherwise activate IFN production. In support, we observed up to 5-fold accumulation of viral DNA when SLX4 knocked-down HeLa cells were infected with HIV-1, as compared to infection of SCR-treated HeLa cells (Figure 5F). Taken together, our experiments identify the targeting of active SLX4 by Vpr to HIV-1 DNA as a viral strategy to avoid innate immune sensing.

The SLX4 Complex Is a Negative Regulator of Spontaneous Type 1 IFN Production

We next investigated whether MUS81, VPRBP, and SLX4 may regulate spontaneous IFN production. To this aim, we measured IFNα, IFNβ, and MxA mRNAs after siRNA-mediated silencing of these SLX4com subunits. We observed that sole silencing of these proteins resulted in upregulation of IFNα, IFNβ, and MxA mRNAs (Figure 6A). In addition, FANCP patient cells ($RA3331^{SLX4-/-}$), but not their SLX4 reconstituted counterpart ($RA3331^{SLX4+/+}$) (Kim et al., 2011), displayed high levels of IFNα, IFNβ, and MxA mRNAs (Figure 6B). In agreement with activation of the IFN signaling pathway in $RA3331^{SLX4-/-}$ cells, we found high levels of interferon regulatory factors (IRF) 3 and 7 as compared to $RA3331^{SLX4+/+}$ (Figure 6C). Concurrently, these cells displayed a decreased susceptibility to infection with a VSV-G-pseudotyped HIV molecular clone harboring a luciferase gene as a reporter (HIV-LUC; Figure 6D). Similar results were obtained using $MEF^{MUS81-/-}$ cells (Figures S6A and S6B). In order to determine whether spontaneous production of type 1 IFN in $MEF^{MUS81-/-}$ may be responsible for the decreased susceptibility to HIV-1 infection, we infected MEF with HIV-LUC in the presence of conditioned medium collected from MEF or $MEF^{MUS81-/-}$ (Figure S6C). Cells treated with the conditioned medium from $MEF^{MUS81-/-}$ caused a 2.5-fold decrease of the susceptibility of MEF to HIV-LUC infection. Preincubating conditioned medium from $MEF^{MUS81-/-}$ cells with mouse neutralizing antibody to IFNβ abrogated the antiviral effect (Figure S6D). Taken together, these experiments indicate that SLX4com subunits are responsible for suppressing spontaneous IFN production.

Finally, to determine whether MUS81 contributes to innate immune signal transduction pathways involved in production of proinflammatory cytokines, we silenced MUS81 in HEK293 reporter cell lines that express the secreted alkaline phosphatase (SEAP) or renilla luciferase (LUC) reporter genes under the control of NF-κB and AP-1 transcription factors, respectively (NF-κB-SEAP and AP-1-LUC). Measurement of reporter gene expression showed an accumulation of SEAP, whereas no change was observed in luciferase activity (Figure S6D). This

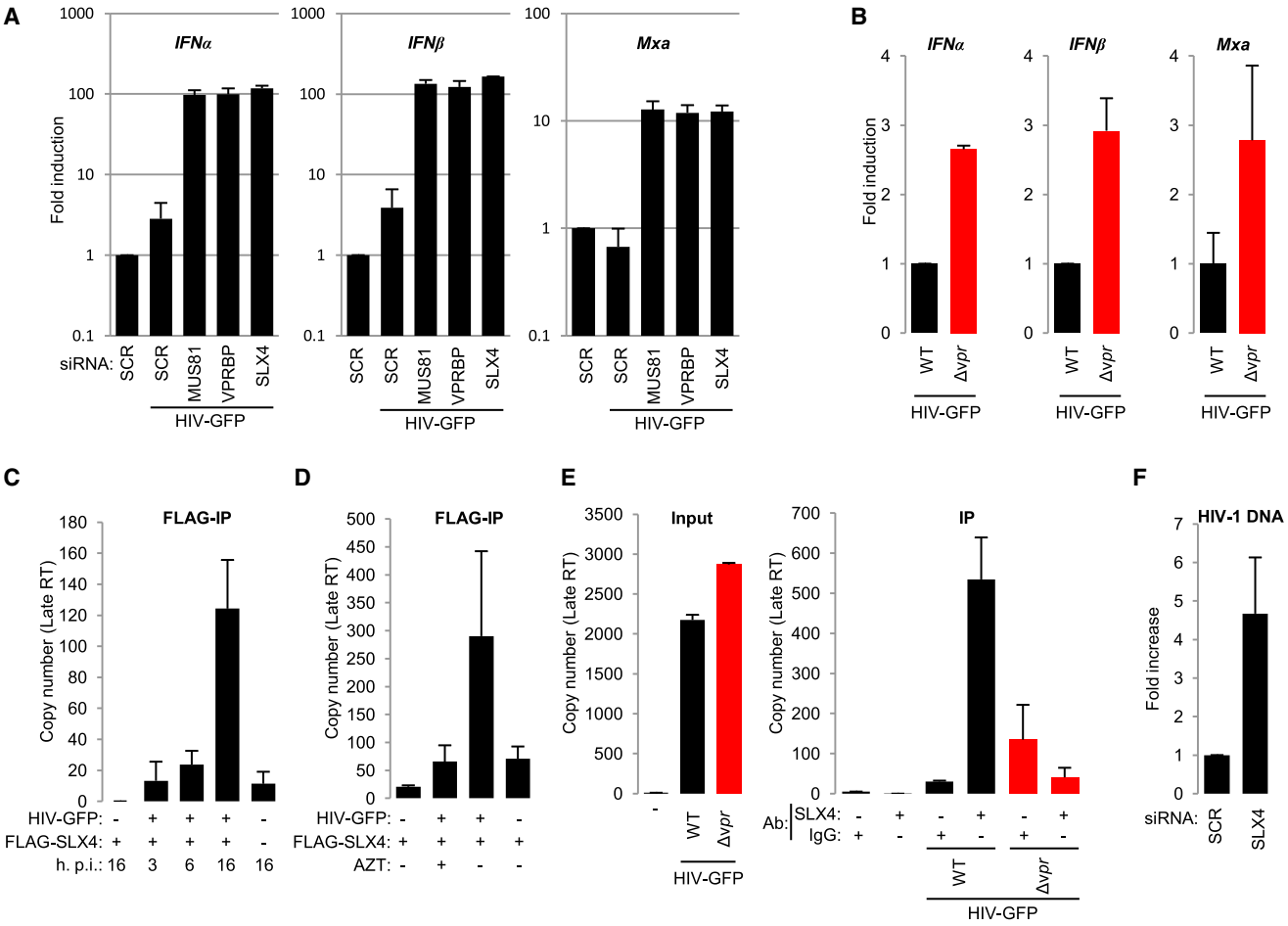

Figure 5. Vpr-Induced SLX4com Manipulation Is Required for Escape of HIV from Innate Immune Sensing

(A) IFNα, IFNβ, and MxA induction were measured by RT-qPCR in HeLa cells transfected with siSCR, siMUS81, siVPRBP, or siSLX4 prior to 48 hr infection with HIV-GFP (n = 3).

(B) HeLa cells were infected for 48 hr with HIV-GFP (WT) or HIVΔVpr-GFP (ΔVpr). Analysis was performed as in (A) (n = 4).

(C) 293T cells overexpressing FLAG-SLX4 were infected with HIV-GFP and harvested at 3, 6, and 16 hr postinfection prior to FLAG-IP and peptide elution. HIV-1 DNA was quantified in eluates by qPCR.

(D) 293T cells were treated as in (C), except that AZT was added at the time of viral infection and cells were harvested 16 hr postinfection. Eluates were analyzed as in (C).

(E) Cells were infected with HIV-GFP or HIVΔVpr-GFP for 16 hr prior to IP using IgG or SLX4-specific antibody. Immunoprecipitates were analyzed as in (C). The left panel shows input DNA. Ab, antibody.

(F) HeLa cells treated with siSCR or siSLX4 were infected for 48 hr with HIV-GFP prior to qPCR quantification of HIV-1 DNA.

See also Figure S5.

indicates that MUS81 specifically prevents activation of the NF-κB signal transduction pathway. Importantly, overexpression of MUS81 did not affect the expression of reporter genes (Figures S6E–S6G), suggesting that MUS81 does not act as an innate immune sensor. Altogether, our data indicate that SLX4com, through the MUS81-EME1 endonuclease, acts as negative regulator of spontaneous production of type 1-IFN.

DISCUSSION

The identity of involved cellular factors, the underlying molecular mechanism, and the functional relevance of Vpr-induced G2/M arrest have been long-standing questions in the HIV field. Here, we show that Vpr interacts with the SLX4 scaffold protein and activates the MUS81-EME1 endonuclease module through recruitment of VPRBP and pPLK1 (Figure 7). In somatic cells, SSE acts as a last resort to process HJ that escape dissolution by Bloom-related helicases. However, because the action of these endonucleases may lead to LOH, resolution of HJ by SSE is tightly regulated. Temporal regulation of Mus81-Mms4^{EME1} activity is achieved through phosphorylation of Mms4^{EME1} by Cdc5^{PLK1} (Gallo-Fernández et al., 2012; Matos et al., 2011; Saugar et al., 2013) or Cdc2^{CDK1} in fission yeast (Dehe et al., 2013). However, untimely or persistent activation

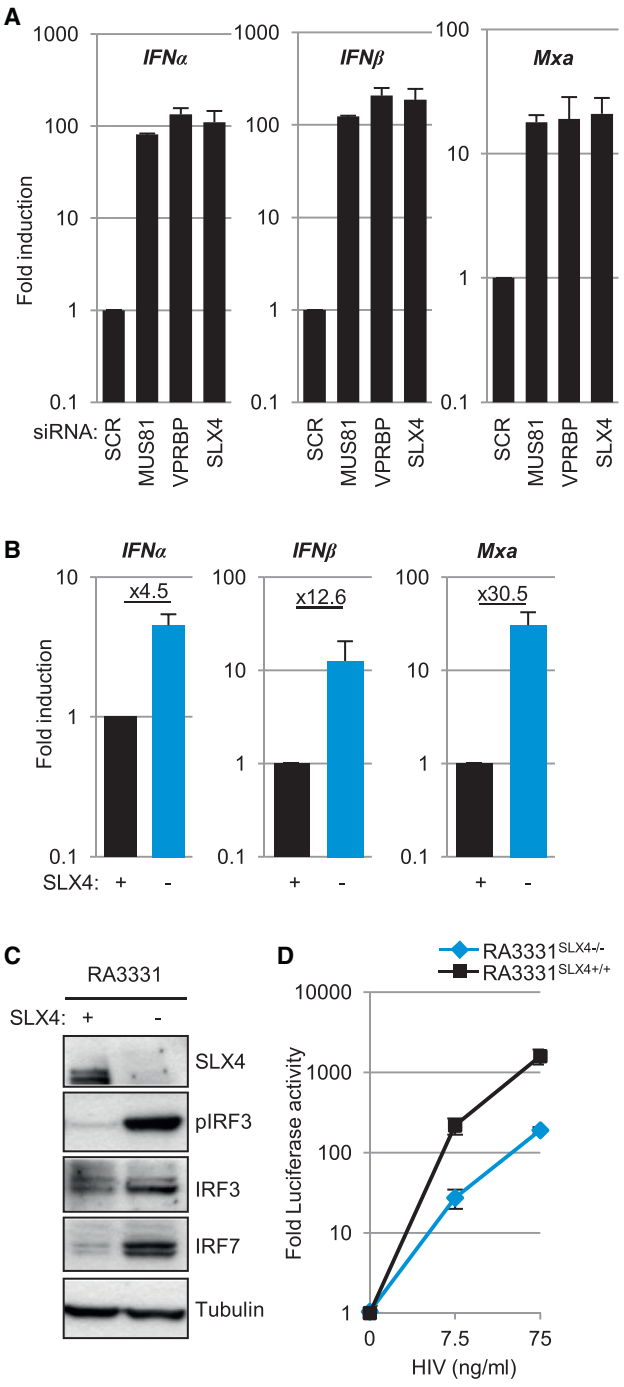

Figure 6. The SLX4 Complex Is a Negative Regulator of Spontaneous Type 1 IFN Production

(A) HeLa cells treated with siSCR, siMUS81, siVPRBP, or siSLX4 prior to analysis as in Figure 5A.

(B) RA3331$^{SLX4-/-}$ cells from FANCP patients complemented or not complemented with SLX4 (RA3331$^{SLX4+/+}$) were analyzed as in Figure 5A (n = 3).

(C) Whole-cell extracts from RA3331$^{SLX4-/-}$ and RA3331$^{SLX4+/+}$ cells were analyzed by WB using indicated antibodies.

(D) RA3331$^{SLX4-/-}$ and RA3331$^{SLX4+/+}$ cells were infected with HIV-LUC for 24 hr. Graph represents mean (± SD) Luciferase activity (n = 3).

See also Figure S6.

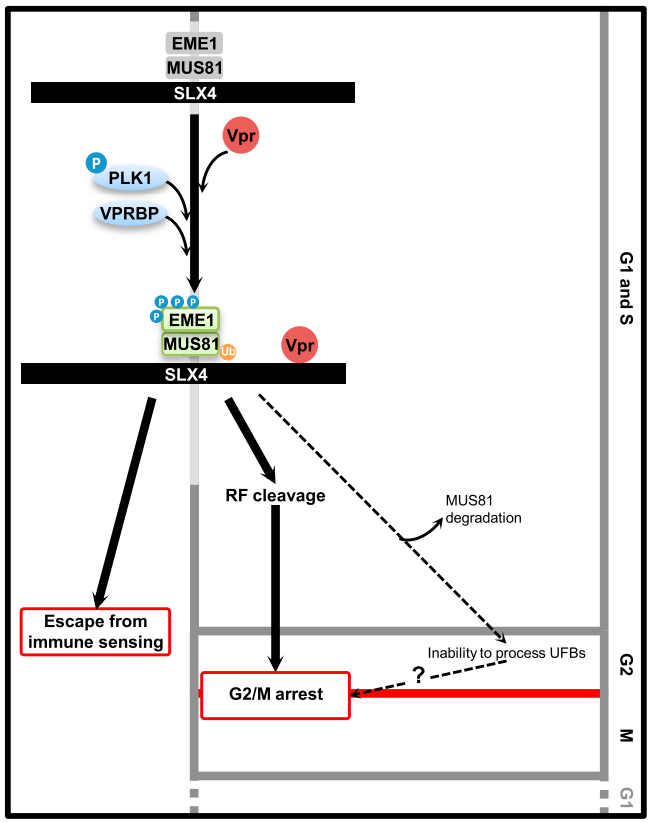

Figure 7. Vpr-Induced Manipulation of the SLX4 Complex

Under physiological conditions, the SLX4com is kept in check during the G1 and S phases of the cell cycle. Expression of Vpr in mammalian cells induces recruitment of pPLK1 and VPRBP to the SLX4com. Subsequently, EME1 is phosphorylated, and MUS81 is ubiquitinated. This results in activation of SLX4-bound MUS81-EME1 molecules and leads to processing of HIV-1 DNA, which contributes to escape from innate immune sensing. Concurrently, cleavage of replication forks (RF) by activated MUS81-EME1 in S phase results in cell-cycle arrest at the G2/M transition. In addition, a decrease in levels of MUS81 may result in the inability of cells to resolve UFBs in G2, which may contribute to G2/M arrest. Nonprocessing of UFBs may lead to genomic instability. Thick arrows represent the prevalent pathway. Question mark indicates the process for which the extent of contribution to Vpr-associated phenotypes is unknown. The red bar represents the G2/M transition.

of this endonuclease complex results in replication stress, including the faulty processing of replication intermediates (Blais et al., 2004; Matos et al., 2013; Szakal and Branzei, 2013).

Here, we show that, in mammalian cells, increased assembly of SLX4 with active MUS81-EME1 and kinase-active PLK1 essentially occurs in mitotic cells. Vpr expression induced premature activation of SLX4-bound MUS81-EME1, suggesting that Vpr causes replication stress. As a testament to ongoing replication stress and activation of the Fanconi anemia pathway (Naim and Rosselli, 2009), we observed an accumulation of FANCD2 foci in Vpr-expressing cells. This is in agreement with the view that Vpr causes cell-cycle arrest through an S-phase-dependent mechanism (Li et al., 2010). Importantly, MUS81-EME1 have been shown to generate DSB by processing stalled replication forks after prolonged replication stress (Hanada et al.,

2007) and are required for the processing of UFBs (Naim et al., 2013; Ying et al., 2013). It is therefore possible to speculate that Vpr expression may lead to abnormal cleavage of replication intermediates by MUS81-EME1 and subsequent accumulation of DSB. Importantly, SLX4 has been identified as a potential ATR substrate (Matsuoka et al., 2007; Mu et al., 2007), and phosphorylation of Eme1 requires $Rad53^{ATR}$ activation (Dehe et al., 2013), a pathway that is activated upon Vpr expression (Roshal et al., 2003); both replication stress and processing of stalled replication forks would ultimately trigger this pathway and result in G2/M arrest (Lobrich and Jeggo, 2007).

An interesting finding from our work is the requirement for VPRBP for Vpr-induced SLX4com activation. This is in agreement with the consensus that posits that interaction of VPRBP with Vpr is a prerequisite for G2/M arrest. We show that Vpr targets MUS81 for ubiquitination by VPRBP, resulting in decreased levels of MUS81. This may be the explanation for the intriguing observation that Vpr expression caused an increase of the number of FANCD2 twin foci in mitotic cells. This is congruent with the recent reports that proteins of the SLX4com, in particular the MUS81-EME1 module, are required to untangle UFBs (Chan et al., 2009; Naim et al., 2013; Wechsler et al., 2011; Ying et al., 2013). Nonetheless, whether ubiquitination of MUS81 is required for SLX4com activation or is involved in regulating active MUS81 levels remains to be investigated. The complete sequence of events leading from SLX4com premature activation to cell-cycle arrest will require further investigations for which we establish Vpr as a powerful molecular tool.

The biological significance of Vpr-mediated G2/M arrest in the context of viral infection remained unclear, as the requirement for Vpr in HIV replication was essentially witnessed in nondividing cells such as macrophages, but not in cycling cells (Casey et al., 2010; Malim and Emerman, 2008). Our data—showing that HIV-1 infection of cells in which SLX4com subunits (SLX4, VPRBP, and MUS81) were knocked down results in type 1 IFN production—suggest that HIV-1 manipulates the SLX4com to avoid triggering innate immune responses. Thus, it is possible that the biological endpoint of Vpr-mediated recruitment of SLX4com to viral DNA and activation of associated MUS81-EME1 is to avoid accumulation of excess viral DNA, thereby preventing its sensing and subsequent type 1 IFN production. In support and in agreement with previous reports (Doehle et al., 2009; Okumura et al., 2008), infection of cells using HIV-1ΔVpr results in increased IFN production as compared to infection with HIV-1. Thus, we suggest that, similar to the exonucleases TREX1 and RNASEH2, the SLX4com helps HIV escape innate immune sensing by processing viral nucleic acid susceptible of inducing type 1 IFN (Rice et al., 2009; Yan et al., 2010). As for TREX1 and RNASEH2, SLX4com subunits do not act as nucleic acid sensors because their overexpression did not lead to IFN production.

Our study unveils the implication of the SLX4com in suppressing type 1 IFN production in the absence of viral infection. Indeed, sole silencing of MUS81, SLX4, and VPRBP caused a production of type1 IFN, induction of ISG, and activation of the NF-κB transcription factor involved in proinflammatory cytokine production, and spontaneous production of type 1 IFN was observed in $RA3331^{SLX4-/-}$ and $MEF^{MUS81-/-}$ cells. This opens the question of the nucleic acid species, which accumulate in the absence of SLX4com that are detected by nucleic acid sensors and lead to production of IFN. Aberrant replication intermediates and/or nucleic acids derived from endogenous retroelements represent possible candidates (Stetson et al., 2008; Yang et al., 2007). The identification of the SLX4com as the target of Vpr that accounts for G2/M cell-cycle arrest opens perspectives in understanding both the function of this viral accessory protein and the involvement of the DNA repair machinery in the complex interaction between viruses and innate immunity.

EXPERIMENTAL PROCEDURES

For detailed experimental procedures, see Supplemental Information.

Purification of Vpr-Associated Complexes

Vpr-associated protein partners were purified from Dignam nuclear extracts derived from 1.5×10^{10} THP-1-iF/H-Vpr or parental THP-1 cells treated with doxycyclin for 11 hr by two-step affinity chromatography according to the standard method (Nakatani and Ogryzko, 2003). Five percent of Flag and HA immunoaffinity-purified F/H-Vpr or mock IPs were resolved on SDS-PAGE and stained with the Silverquest kit (Invitrogen). Remainder eluates were stained with Coomassie-R250. Individual bands or regions of the gel were excised and analyzed by MS at the Harvard Medical School Taplin Biological Mass Spectrometry facility.

In Vitro Cleavage Assay

γ^{32}P radiolabeled 3′ flap and X26 substrates preparation is described in Constantinou et al. (2002). Approximately 30 ng of immunopurified bead-bound FLAG-SLX4 or mock immunoprecipitate was incubated for 30 min at 37°C with ~1 nM substrate in reaction buffer (20 nM Tris [pH7.5], 50 mM NaCl, 10 mM $MgCl_2$, 1 mM $MnCl_2$, 0.1 mg/ml BSA, and 10 mM β-mercaptoethanol). The reaction was stopped by the addition of 20 mM EDTA. Proteinase K and SDS were added to a final concentration of 2 mg/ml and 0.4%, respectively, for 15 min at 37°C. Cleavage efficiency was measured by autoradiography after separation of samples on Tris Borate Ethylamide 8% acrylamide gels.

Analysis of the IFN Pathway

IFNα, IFNβ, and Mxa mRNA were quantified by RT-qPCR using specific probes. Normalization was performed using GAPDH-specific probes. Infections were performed with 0.1 μg/ml p24 of HIV/HIVΔVpr.

NF-κB and AP-1 activity was measured in reporter HEK293 cells lines using the SEAP reporter or Renilla luciferase reporter kits from Invitrogen and Promega, respectively.

SUPPLEMENTAL INFORMATION

Supplemental Information includes Extended Experimental Procedures and six figures and can be found with this article online at http://dx.doi.org/10.1016/j.cell.2013.12.011.

ACKNOWLEDGMENTS

We thank members of the Molecular Virology lab for critical reading of the manuscript, K.J. Patel for $MEF^{SLX4-/-}$ cells, A. Smogorzewska for $RA3331^{SLX4-/-}$ and $RA3331^{SLX4+/+}$ cells, R. Hakem for $MEF^{MUS81-/-}$ cells, W. Harper for HIS_6-tagged proteins and FLAG-tagged SLX4, and I. Poser for the BAC modification cassette and HeLa Kyoto cells. We are grateful to Montpellier RIO Imaging for help with the microscopy analyses. This work was supported by ERC (250333), SIDACTION (Fonds de dotation PIERRE BERGE), ANRS, and European FP7 "HIT HIDDEN HIV" (305762). Work in the laboratory of A.C. was supported by "la Fondation ARC pour la Recherche sur le Cancer" (8604XA1020T). P.H. and A.Y. were supported by SIDACTION and FRM, respectively.

Received: April 26, 2013
Revised: September 5, 2013
Accepted: December 10, 2013
Published: January 9, 2014

REFERENCES

Beck, H., Nähse-Kumpf, V., Larsen, M.S., O'Hanlon, K.A., Patzke, S., Holmberg, C., Mejlvang, J., Groth, A., Nielsen, O., Syljuåsen, R.G., and Sørensen, C.S. (2012). Cyclin-dependent kinase suppression by WEE1 kinase protects the genome through control of replication initiation and nucleotide consumption. Mol. Cell. Biol. *32*, 4226–4236.

Belzile, J.P., Duisit, G., Rougeau, N., Mercier, J., Finzi, A., and Cohen, E.A. (2007). HIV-1 Vpr-mediated G2 arrest involves the DDB1-CUL4AVPRBP E3 ubiquitin ligase. PLoS Pathog. *3*, e85.

Blais, V., Gao, H., Elwell, C.A., Boddy, M.N., Gaillard, P.H., Russell, P., and McGowan, C.H. (2004). RNA interference inhibition of Mus81 reduces mitotic recombination in human cells. Mol. Biol. Cell *15*, 552–562.

Casey, L., Wen, X., and de Noronha, C.M. (2010). The functions of the HIV1 protein Vpr and its action through the DCAF1.DDB1.Cullin4 ubiquitin ligase. Cytokine *51*, 1–9.

Chan, K.L., Palmai-Pallag, T., Ying, S., and Hickson, I.D. (2009). Replication stress induces sister-chromatid bridging at fragile site loci in mitosis. Nat. Cell Biol. *11*, 753–760.

Constantinou, A., Chen, X.B., McGowan, C.H., and West, S.C. (2002). Holliday junction resolution in human cells: two junction endonucleases with distinct substrate specificities. EMBO J. *21*, 5577–5585.

Davy, C., and Doorbar, J. (2007). G2/M cell cycle arrest in the life cycle of viruses. Virology *368*, 219–226.

DeHart, J.L., Zimmerman, E.S., Ardon, O., Monteiro-Filho, C.M., Argañaraz, E.R., and Planelles, V. (2007). HIV-1 Vpr activates the G2 checkpoint through manipulation of the ubiquitin proteasome system. Virol. J. *4*, 57.

Dehe, P.M., Coulon, S., Scaglione, S., Shanahan, P., Takedachi, A., Wohlschlegel, J.A., Yates, J.R., 3rd, Llorente, B., Russell, P., and Gaillard, P.H. (2013). Regulation of Mus81-Eme1 Holliday junction resolvase in response to DNA damage. Nat. Struct. Mol. Biol. *20*, 598–603.

Di Marzio, P., Choe, S., Ebright, M., Knoblauch, R., and Landau, N.R. (1995). Mutational analysis of cell cycle arrest, nuclear localization and virion packaging of human immunodeficiency virus type 1 Vpr. J. Virol. *69*, 7909–7916.

Doehle, B.P., Hladik, F., McNevin, J.P., McElrath, M.J., and Gale, M., Jr. (2009). Human immunodeficiency virus type 1 mediates global disruption of innate antiviral signaling and immune defenses within infected cells. J. Virol. *83*, 10395–10405.

Fagerlie, S.R., Koretsky, T., Torok-Storb, B., and Bagby, G.C. (2004). Impaired type I IFN-induced Jak/STAT signaling in FA-C cells and abnormal CD4+ Th cell subsets in Fancc-/- mice. J. Immunol. *173*, 3863–3870.

Fekairi, S., Scaglione, S., Chahwan, C., Taylor, E.R., Tissier, A., Coulon, S., Dong, M.Q., Ruse, C., Yates, J.R., 3rd, Russell, P., et al. (2009). Human SLX4 is a Holliday junction resolvase subunit that binds multiple DNA repair/recombination endonucleases. Cell *138*, 78–89.

Fugger, K., Chu, W.K., Haahr, P., Kousholt, A.N., Beck, H., Payne, M.J., Hanada, K., Hickson, I.D., and Sørensen, C.S. (2013). FBH1 co-operates with MUS81 in inducing DNA double-strand breaks and cell death following replication stress. Nat. Commun. *4*, 1423.

Gallo-Fernández, M., Saugar, I., Ortiz-Bazán, M.A., Vázquez, M.V., and Tercero, J.A. (2012). Cell cycle-dependent regulation of the nuclease activity of Mus81-Eme1/Mms4. Nucleic Acids Res. *40*, 8325–8335.

Hanada, K., Budzowska, M., Davies, S.L., van Drunen, E., Onizawa, H., Beverloo, H.B., Maas, A., Essers, J., Hickson, I.D., and Kanaar, R. (2007). The structure-specific endonuclease Mus81 contributes to replication restart by generating double-strand DNA breaks. Nat. Struct. Mol. Biol. *14*, 1096–1104.

He, J., Choe, S., Walker, R., Di Marzio, P., Morgan, D.O., and Landau, N.R. (1995). Human immunodeficiency virus type 1 viral protein R (Vpr) arrests cells in the G2 phase of the cell cycle by inhibiting p34cdc2 activity. J. Virol. *69*, 6705–6711.

Hrecka, K., Gierszewska, M., Srivastava, S., Kozaczkiewicz, L., Swanson, S.K., Florens, L., Washburn, M.P., and Skowronski, J. (2007). Lentiviral Vpr usurps Cul4-DDB1[VprBP] E3 ubiquitin ligase to modulate cell cycle. Proc. Natl. Acad. Sci. USA *104*, 11778–11783.

Jowett, J.B., Planelles, V., Poon, B., Shah, N.P., Chen, M.L., and Chen, I.S. (1995). The human immunodeficiency virus type 1 vpr gene arrests infected T cells in the G2 + M phase of the cell cycle. J. Virol. *69*, 6304–6313.

Kim, Y., Lach, F.P., Desetty, R., Hanenberg, H., Auerbach, A.D., and Smogorzewska, A. (2011). Mutations of the SLX4 gene in Fanconi anemia. Nat. Genet. *43*, 142–146.

Kim, Y., Spitz, G.S., Veturi, U., Lach, F.P., Auerbach, A.D., and Smogorzewska, A. (2013). Regulation of multiple DNA repair pathways by the Fanconi anemia protein SLX4. Blood *121*, 54–63.

Lai, M., Zimmerman, E.S., Planelles, V., and Chen, J. (2005). Activation of the ATR pathway by human immunodeficiency virus type 1 Vpr involves its direct binding to chromatin in vivo. J. Virol. *79*, 15443–15451.

Le Rouzic, E., Belaïdouni, N., Estrabaud, E., Morel, M., Rain, J.C., Transy, C., and Margottin-Goguet, F. (2007). HIV1 Vpr arrests the cell cycle by recruiting DCAF1/VprBP, a receptor of the Cul4-DDB1 ubiquitin ligase. Cell Cycle *6*, 182–188.

Li, G., Park, H.U., Liang, D., and Zhao, R.Y. (2010). Cell cycle G2/M arrest through an S phase-dependent mechanism by HIV-1 viral protein R. Retrovirology *7*, 59.

Lobrich, M., and Jeggo, P.A. (2007). The impact of a negligent G2/M checkpoint on genomic instability and cancer induction. Nat. Rev. Cancer *7*, 861–869.

Malim, M.H., and Emerman, M. (2008). HIV-1 accessory proteins—ensuring viral survival in a hostile environment. Cell Host Microbe *3*, 388–398.

Matos, J., Blanco, M.G., Maslen, S., Skehel, J.M., and West, S.C. (2011). Regulatory control of the resolution of DNA recombination intermediates during meiosis and mitosis. Cell *147*, 158–172.

Matos, J., Blanco, M.G., and West, S.C. (2013). Cell-cycle kinases coordinate the resolution of recombination intermediates with chromosome segregation. Cell Rep. *4*, 76–86.

Matsuoka, S., Ballif, B.A., Smogorzewska, A., McDonald, E.R., 3rd, Hurov, K.E., Luo, J., Bakalarski, C.E., Zhao, Z., Solimini, N., Lerenthal, Y., et al. (2007). ATM and ATR substrate analysis reveals extensive protein networks responsive to DNA damage. Science *316*, 1160–1166.

Mu, J.J., Wang, Y., Luo, H., Leng, M., Zhang, J., Yang, T., Besusso, D., Jung, S.Y., and Qin, J. (2007). A proteomic analysis of ataxia telangiectasia-mutated (ATM)/ATM-Rad3-related (ATR) substrates identifies the ubiquitin-proteasome system as a regulator for DNA damage checkpoints. J. Biol. Chem. *282*, 17330–17334.

Muñoz, I.M., Hain, K., Déclais, A.C., Gardiner, M., Toh, G.W., Sanchez-Pulido, L., Heuckmann, J.M., Toth, R., Macartney, T., Eppink, B., et al. (2009). Coordination of structure-specific nucleases by human SLX4/BTBD12 is required for DNA repair. Mol. Cell *35*, 116–127.

Naim, V., and Rosselli, F. (2009). The FANC pathway and BLM collaborate during mitosis to prevent micro-nucleation and chromosome abnormalities. Nat. Cell Biol. *11*, 761–768.

Naim, V., Wilhelm, T., Debatisse, M., and Rosselli, F. (2013). ERCC1 and MUS81-EME1 promote sister chromatid separation by processing late replication intermediates at common fragile sites during mitosis. Nat. Cell Biol. *15*, 1008–1015.

Nakatani, Y., and Ogryzko, V. (2003). Immunoaffinity purification of mammalian protein complexes. Methods Enzymol. *370*, 430–444.

Okumura, A., Alce, T., Lubyova, B., Ezelle, H., Strebel, K., and Pitha, P.M. (2008). HIV-1 accessory proteins VPR and Vif modulate antiviral response by targeting IRF-3 for degradation. Virology *373*, 85–97.

Poon, B., Jowett, J.B., Stewart, S.A., Armstrong, R.W., Rishton, G.M., and Chen, I.S. (1997). Human immunodeficiency virus type 1 vpr gene induces phenotypic effects similar to those of the DNA alkylating agent, nitrogen mustard. J. Virol. *71*, 3961–3971.

Re, F., Braaten, D., Franke, E.K., and Luban, J. (1995). Human immunodeficiency virus type 1 Vpr arrests the cell cycle in G2 by inhibiting the activation of p34cdc2-cyclin B. J. Virol. *69*, 6859–6864.

Rice, G.I., Bond, J., Asipu, A., Brunette, R.L., Manfield, I.W., Carr, I.M., Fuller, J.C., Jackson, R.M., Lamb, T., Briggs, T.A., et al. (2009). Mutations involved in Aicardi-Goutières syndrome implicate SAMHD1 as regulator of the innate immune response. Nat. Genet. *41*, 829–832.

Rogel, M.E., Wu, L.I., and Emerman, M. (1995). The human immunodeficiency virus type 1 vpr gene prevents cell proliferation during chronic infection. J. Virol. *69*, 882–888.

Roshal, M., Kim, B., Zhu, Y., Nghiem, P., and Planelles, V. (2003). Activation of the ATR-mediated DNA damage response by the HIV-1 viral protein R. J. Biol. Chem. *278*, 25879–25886.

Saugar, I., Vázquez, M.V., Gallo-Fernández, M., Ortiz-Bazán, M.A., Segurado, M., Calzada, A., and Tercero, J.A. (2013). Temporal regulation of the Mus81-Mms4 endonuclease ensures cell survival under conditions of DNA damage. Nucleic Acids Res. *41*, 8943–8958.

Schwartz, E.K., and Heyer, W.D. (2011). Processing of joint molecule intermediates by structure-selective endonucleases during homologous recombination in eukaryotes. Chromosoma *120*, 109–127.

Sengerová, B., Wang, A.T., and McHugh, P.J. (2011). Orchestrating the nucleases involved in DNA interstrand cross-link (ICL) repair. Cell Cycle *10*, 3999–4008.

Stetson, D.B., Ko, J.S., Heidmann, T., and Medzhitov, R. (2008). Trex1 prevents cell-intrinsic initiation of autoimmunity. Cell *134*, 587–598.

Svendsen, J.M., and Harper, J.W. (2010). GEN1/Yen1 and the SLX4 complex: Solutions to the problem of Holliday junction resolution. Genes Dev. *24*, 521–536.

Svendsen, J.M., Smogorzewska, A., Sowa, M.E., O'Connell, B.C., Gygi, S.P., Elledge, S.J., and Harper, J.W. (2009). Mammalian BTBD12/SLX4 assembles a Holliday junction resolvase and is required for DNA repair. Cell *138*, 63–77.

Szakal, B., and Branzei, D. (2013). Premature Cdk1/Cdc5/Mus81 pathway activation induces aberrant replication and deleterious crossover. EMBO J. *32*, 1155–1167.

Tachiwana, H., Shimura, M., Nakai-Murakami, C., Tokunaga, K., Takizawa, Y., Sata, T., Kurumizaka, H., and Ishizaka, Y. (2006). HIV-1 Vpr induces DNA double-strand breaks. Cancer Res. *66*, 627–631.

Tan, L., Ehrlich, E., and Yu, X.F. (2007). DDB1 and Cul4A are required for human immunodeficiency virus type 1 Vpr-induced G2 arrest. J. Virol. *81*, 10822–10830.

Tristem, M., Marshall, C., Karpas, A., and Hill, F. (1992). Evolution of the primate lentiviruses: evidence from vpx and vpr. EMBO J. *11*, 3405–3412.

Wechsler, T., Newman, S., and West, S.C. (2011). Aberrant chromosome morphology in human cells defective for Holliday junction resolution. Nature *471*, 642–646.

Wen, X., Duus, K.M., Friedrich, T.D., and de Noronha, C.M. (2007). The HIV1 protein Vpr acts to promote G2 cell cycle arrest by engaging a DDB1 and Cullin4A-containing ubiquitin ligase complex using VprBP/DCAF1 as an adaptor. J. Biol. Chem. *282*, 27046–27057.

Wu, L., and Hickson, I.D. (2003). The Bloom's syndrome helicase suppresses crossing over during homologous recombination. Nature *426*, 870–874.

Yan, N., Regalado-Magdos, A.D., Stiggelbout, B., Lee-Kirsch, M.A., and Lieberman, J. (2010). The cytosolic exonuclease TREX1 inhibits the innate immune response to human immunodeficiency virus type 1. Nat. Immunol. *11*, 1005–1013.

Yang, Y.G., Lindahl, T., and Barnes, D.E. (2007). Trex1 exonuclease degrades ssDNA to prevent chronic checkpoint activation and autoimmune disease. Cell *131*, 873–886.

Ying, S., Minocherhomji, S., Chan, K.L., Palmai-Pallag, T., Chu, W.K., Wass, T., Mankouri, H.W., Liu, Y., and Hickson, I.D. (2013). MUS81 promotes common fragile site expression. Nat. Cell Biol. *15*, 1001–1007.

Zhao, L.J., Mukherjee, S., and Narayan, O. (1994). Biochemical mechanism of HIV-I Vpr function. Specific interaction with a cellular protein. J. Biol. Chem. *269*, 15577–15582.

Zimmerman, E.S., Chen, J., Andersen, J.L., Ardon, O., Dehart, J.L., Blackett, J., Choudhary, S.K., Camerini, D., Nghiem, P., and Planelles, V. (2004). Human immunodeficiency virus type 1 Vpr-mediated G2 arrest requires Rad17 and Hus1 and induces nuclear BRCA1 and gamma-H2AX focus formation. Mol. Cell. Biol. *24*, 9286–9294.